Computational Mechanics 31 (2003) 479–488 © Springer-Verlag 2003
DOI 10.1007/s00466-003-0454-z

On the numerical integration of a class of pressure-dependent plasticity models including kinematic hardening

U. Mühlich, W. Brocks

Abstract The algorithm proposed by Aravas to integrate a special type of elastic-plastic constitutive equations has been extended to incorporate kinematic hardening. Like in the case of isotropic hardening, the number of primary unknowns for the Newton iteration can be reduced to two scalar strain variables. Furthermore, the consistent tangent can be obtained explicitly. The modified algorithm has been applied to a Gurson-type model which takes into account kinematic hardening and the predictions of the Gurson-like model are compared with results obtained by unit cell calculations.

1 Introduction

To solve problems of elastoplasticity using finite element method, the constitutive equations have to be integrated for every time increment at each Gauss-point. If an implicit integration scheme is used, a system of n nonlinear equations has to be solved and a so-called consistent tangent has to be calculated to ensure quadratic convergence of the global equilibrium iteration. The number of equations (n) depends on the considered constitutive model. Here, the attention is focused on constitutive models with pressure dependent yield condition and flow rule including kinematic hardening. Rate independent elastoplasticity is considered.

Because n effects directly the analysis time, it is always usefull to reduce n as much as possible. A first reduction can be reached if the radial return algorithm proposed in [1] is applied. According to the structure of the constitutive model, further reduction of n may be possible by algebraic operations as it was done for example in [2] for elasto-plasticity and viscoplasticity with kinematic hardening.

A reduction of n cannot be reached in the way described in [2] if constitutive models with pressure dependent yield condition and flow rule are considered. On the other hand, a integration algorithm for such models was developed by Aravas [3], whereby isotropic hardening was considered. The algorithm makes use of the radial return algorithm and applies the Newton-Raphson method to solve the system of nonlinear equations. No further effort was made in [3] to reduce n by algebraic operations but when the Newton-Raphson method was applied, the number of primary unknowns involved in iteration has been reduced to two.

The algorithm proposed in [3] can be extended to kinematic hardening. The number of primary unknowns for the Newton-Raphson method can be reduced to two like in the case of isotropic hardening and the consistent tangent can be given explicitly.

The integration procedure proposed here was developed with the aim to apply it for the implementation of continumm damage models as user-supplied subroutine into the finite element program Abaqus [4]. The corresponding continuum mechanics framework is discussed briefly in Sect. 2. The general structure of the constitutive equations which are considered here is presented in Sect. 3. The extension of the integration algorithm proposed in [3] to kinematic hardening is described in Sect. 4. In Sect. 5 the extended algorithm is applied to a Gurson-type model which takes into account kinematic hardening. The predictions of the Gurson-type model will be compared with the results obtained by unit cell calculations in Sect. 6.

2 Preliminaries

In the following, boldface symbols denote tensors, the order of which is indicated by the context. Underlined letters are used for vectors. The summation convention is used for Latin and Greek indices unless otherwise indicated. With respect to Latin indices the summation is carried out from one to three. In the case of Greek indices the summation is carried out from one up to the number of internal variables H_α. The differentiation of a variable a_i with respect to the spatial coordinate x_j is denoted by

$$a_{i,j} := \frac{\partial a_i}{\partial x_j} \quad . \tag{1}$$

The concept of kinematics considered here is based on the commonly used polar decomposition of the deformation gradient $\mathbf{F}$ into elastic and plastic part

$$\mathbf{F} = \mathbf{F}^{el}\mathbf{F}^{pl} \quad . \tag{2}$$

Received: 25 March 2002 / Accepted: 19 May 2003

U. Mühlich
Universidad Técnica Federico Santa María,
Departamento de Ciencias Materiales,
Avenida España 1680, Casilla 110-VM, Valparaíso, Chile

W. Brocks (✉)
Institut für Werkstoffforschung – WMS, GKSS
Forschungszentrum Geesthacht, 21502 Geesthacht, FRG

The authors acknowledge the financial support from DFG-Project Br 521/11-3. Furthermore, the authors are grateful to Jean-Baptiste Leblond from the Université Pierre et Marie Curie, Paris for several helpful suggestions and hints.

From the velocity gradient

$$\mathbf{L} = \left(\frac{\partial \underline{v}}{\partial \underline{x}}\right) \tag{3}$$

the strain rates

$$\dot{\mathbf{E}} = \tfrac{1}{2}\left(\mathbf{L} + \mathbf{L}^{\mathrm{T}}\right) \tag{4}$$

and the spin rates

$$\mathbf{W} = \tfrac{1}{2}\left(\mathbf{L} - \mathbf{L}^{\mathrm{T}}\right) \tag{5}$$

are derived, where $\underline{v}$ is the actual velocity of a point, $\underline{x}$ its actual spatial position and the superscript **T** indicates the transposed quantity. If the total principal elastic strains are small compared to unity, the additive strain rate decomposition

$$\dot{\mathbf{E}} = \dot{\mathbf{E}}^{\mathrm{el}} + \dot{\mathbf{E}}^{\mathrm{pl}} \tag{6}$$

is an admissible approximation. The total strains are obtained by time integration using the Hughes-Winget approach given in [5]. Therefore, the integrated equation

$$\mathbf{E} = \mathbf{E}^{\mathrm{el}} + \mathbf{E}^{\mathrm{pl}} \tag{7}$$

also consists of objective measures, whereby the algorithm proposed in [5] only ensures weak objectivity. Furthermore, application of the Hughes-Winget approach requieres application of the Jaumann rate

$$\overset{\triangledown}{()} = \dot{()} + ()\mathbf{W} - \mathbf{W}() \tag{8}$$

with respect to the stress quantities included in the constitutive equations (see for example [6]). Here, the strain rates (4), the Cauchy stress tensor and its Jaumann derivate are used to formulate the constitutive equations. The foregoing discussed framework limits the application of the integration procedure for kinematic hardening which is proposed here to small total strains and large rotations. For large plastic strains and kinematic hardening, more sophisticated concepts have to be applied (see for example [7] for more detailed information). In order to present the equations transparently for computer codification, the index notation is prefered in the following.

3 Constitutive equations

With respect to the material behaviour, two different regimes are distinguished by the scalar valued yield function Φ.

$$\Phi = \Phi(\mathbf{S}, H_\alpha) \tag{9}$$

where **S** denotes the difference between the Cauchy stress tensor, Σ, and the backstress tensor **A**

$$\mathbf{S} = \Sigma - \mathbf{A} \ . \tag{10}$$

The backstresses A_{ij} are used to take into account kinematic hardening. Isotropic hardening, damage etc. is described by the variables H_α. If the condition

$$\Phi(\mathbf{S}\ , H_\alpha) = 0 \quad \wedge \quad \overset{\triangledown}{\Sigma}_{ij} \frac{\partial \Phi}{\partial \Sigma_{ij}}\bigg|_{H_\alpha, A_{kl}=\mathrm{const}} \geq 0 \tag{11}$$

is fulfilled, elastic–plastic material behaviour is assumed, else linear elasticity is applied which means that

$$\Sigma_{ij} = C^{\mathrm{el}}_{ijkl} E^{\mathrm{el}}_{kl} \ , \tag{12}$$

where the C_{ijkl} are the components of the elasticity tensor

$$C_{ijkl} = G I_{ijkl} + (K - \tfrac{2}{3}G)\delta_{ij}\delta_{kl} \ , \tag{13}$$

written by means of the bulk modulus K and the shear modulus G. The fourth order unit tensor I_{ijkl} is given by

$$I_{ijkl} = \tfrac{1}{2}\left(\delta_{ik}\delta_{jl} + \delta_{il}\delta_{jk}\right) \ . \tag{14}$$

Here, yield conditions having the following general structure

$$\Phi = \Phi(\bar{Q}, \bar{P}, H_\alpha) = 0 \tag{15}$$

are considered with

$$\bar{Q} = \sqrt{\tfrac{3}{2} S'_{ij} S'_{ij}} \tag{16}$$

$$\bar{P} = -\tfrac{1}{3} S_{mm} \tag{17}$$

where the S'_{ij} are the components of the deviatoric part of **S**. In the following the elastic–plastic regime is considered. It is assumed that the plastic strain rates are given by a flow rule like

$$\dot{E}^{\mathrm{pl}}_{ij} = \dot{\Lambda} \frac{\partial F(\bar{Q}, \bar{P}, H_\alpha)}{\partial \Sigma_{ij}} \tag{18}$$

where $\dot{\Lambda}$ denotes the so-called plastic multiplier and F denotes the plastic potential. F is a scalar valued function with a structure similar to that of Φ. If an associated flow rule is assumed, Φ and F are identical. The flow rule (18) can be written as

$$\dot{E}^{\mathrm{pl}}_{ij} = \dot{\Lambda}\left(\frac{\partial F}{\partial \bar{Q}} \bar{N}_{ij} - \frac{\partial F}{\partial \bar{P}} \delta_{ij}\right) \tag{19}$$

with

$$\bar{N}_{ij} = \frac{3}{2} \frac{\Sigma'_{ij} - A'_{ij}}{\bar{Q}} \ . \tag{20}$$

Following Aravas [3], the two scalar strain variables

$$\dot{E}_P = -\dot{\Lambda} \frac{\partial F}{\partial \bar{P}} \ , \tag{21}$$

$$\dot{E}_Q = \dot{\Lambda} \frac{\partial F}{\partial \bar{Q}} \tag{22}$$

are defined. Introducing (21) and (22) into (19) gives

$$\dot{E}^{\mathrm{pl}}_{ij} = \tfrac{1}{3}\dot{E}_P \delta_{ij} + \dot{E}_Q \bar{N}_{ij} \ . \tag{23}$$

Elimination of the plastic multiplier $\dot{\Lambda}$ from (21) and (22) leads to

$$\dot{E}_P \frac{\partial F}{\partial \bar{Q}} + \dot{E}_Q \frac{\partial F}{\partial \bar{P}} = 0 \ . \tag{24}$$

It is assumed that the evolution of the internal variables H_α is given by

$$\dot{H}_\alpha = H_\alpha(\mathbf{E}^{\mathrm{pl}}, \mathbf{S}, H_\beta) \ . \tag{25}$$

The plasticity model is completely defined by introducing evolution equations for the backstresses

$$\overset{\triangledown}{A}_{ij} = a_{ij}(\mathbf{E}^{pl}, \mathbf{S}, H_\beta) \ . \tag{26}$$

Here, rate independent constitutive models are considered. Therefore, (25) and (26) cannot be chosen arbitrarily but have to be homogeneous in time. Finally, it follows from (12) and (7) that

$$\Sigma_{ij} = C_{ijkl}(E_{kl} - E^{pl}_{kl}) \ . \tag{27}$$

Within the elastic–plastic regime the following set of $20 + \alpha$ nonlinear algebraic and differential equations can be used to determine the $20 + \alpha$ unknowns Σ_{ij}, E^{pl}_{ij}, E_P, E_Q, H_α, A_{ij}

$$\begin{aligned}
&\Phi(\bar{Q}, \bar{P}, H_\alpha) = 0 \\
&\Sigma_{ij} = C_{ijkl}(E_{kl} - E^{pl}_{kl}) \\
&\dot{E}^{pl}_{ij} = \tfrac{1}{3}\dot{E}_P \delta_{ij} + \dot{E}_Q \bar{N}_{ij} \\
&\dot{E}_P \frac{\partial F}{\partial \bar{Q}} + \dot{E}_Q \frac{\partial F}{\partial \bar{P}} = 0 \\
&\dot{H}_\alpha = H_\alpha(\mathbf{E}^{pl}, \mathbf{S}, H_\beta) \\
&\overset{\triangledown}{A}_{ij} = a_{ij}(\mathbf{E}^{pl}, \mathbf{S}, H_\beta)
\end{aligned} \tag{28}$$

if all quantities are given at time t and the total strain rates are known.

4 Numerical integration of the constitutive equations

4.1 Description of the method

A predictor corrector method (radial return) together with Euler's implicit integration procedure is used for the numerical integration. The value of a quantity f at time t is denoted by ${}^t f$ and at time $t + \triangle t$ by ${}^{t+\triangle t} f$, respectively. The discrete time increment $\triangle t$ as well as ${}^t f$ are known. Furthermore it is assumed that the total strain increments ΔE_{ij} are given. Using Euler's implicit integration method, ${}^{t+\triangle t} f$ is determined approximately by

$${}^{t+\triangle t} f = {}^t f + {}^{t+\triangle t}\dot{f} \triangle t \tag{29}$$

which is equivalent to

$$\triangle f = {}^{t+\triangle t}\dot{f} \triangle t \tag{30}$$

if the notation $\triangle f = {}^{t+\triangle t} f - {}^t f$ is used. In order to simplify the notation, the supscript $t + \triangle t$ will be dropped, with the understanding that all quantities are evaluated at $t + \triangle t$, unless otherwise indicated.

Application of the implicit time integration to (6) and (23) leads to

$$\triangle E_{ij} = \triangle E^{el}_{ij} + \triangle E^{pl}_{ij} \ , \tag{31}$$

$$\triangle E^{pl}_{ij} = \tfrac{1}{3} \triangle E_P \delta_{ij} + \triangle E_Q \bar{N}_{ij} \ . \tag{32}$$

Using (12), (31) and (32), the stress state at the end of the time increment can be written as

$$\Sigma_{ij} = \Sigma^{pred}_{ij} - K \triangle E_P \delta_{ij} - 2G \triangle E_Q \bar{N}_{ij} \tag{33}$$

where

$$\Sigma^{pred}_{ij} = C_{ijkl}({}^t E^{el}_{kl} + \triangle E_{kl}) \tag{34}$$

is the so-called elastic predictor state. The deviatoric stress state is then given by

$$\Sigma'_{ij} = \Sigma'^{pred}_{ij} - 2G \triangle E_Q \bar{N}_{ij} \ . \tag{35}$$

From (35) and (20) it follows that

$$\bar{N}_{ij} = \frac{3}{2} \frac{\Sigma'^{pred}_{ij} - A'_{ij}}{\sqrt{\frac{3}{2}(\Sigma'^{pred}_{kl} - A'_{kl})(\Sigma'^{pred}_{kl} - A'_{kl})}} \tag{36}$$

so that the $\bar{N}_{ij}$ are fully determined by the elastic predictor state and the values of the A'_{ij} at time $t + \Delta t$ and therefore also the stress state at $t + \Delta t$ is fully defined in the same way (see (33)), which means that the stresses Σ_{ij} are no longer primary unknowns but functions of ΔE_P, ΔE_Q, A_{ij} and H_α. Therefore $\bar{P}$ and $\bar{Q}$ can be expressed completely by ΔE_P, ΔE_Q, A_{ij} and H_α. Using (33), (17) and (16) can be written as

$$\bar{P} = -\frac{1}{3}\Sigma^{pred}_{kk} + \frac{1}{3} A_{kk} + K \Delta E_P \tag{37}$$

$$\bar{Q} = \sqrt{\frac{3}{2}\left(\Sigma'^{pred}_{ij} - A'_{ij}\right)\left(\Sigma'^{pred}_{ij} - A'_{ij}\right)} - 3G \Delta E_Q \ . \tag{38}$$

Application of the implicit integration scheme (29) to (25) and (26) gives

$$\Delta H_\alpha = \bar{h}_\alpha(\Delta E_P, \Delta E_Q, H_\beta, A_{kl}) \tag{39}$$

and

$$\Delta A_{ij} = \bar{a}_{ij}(\Delta E_P, \Delta E_Q, H_\beta, A_{kl}) \ , \tag{40}$$

respectively. The notations $\bar{h}_\alpha$ and $\bar{a}_{ij}$ are used for the incremental forms of h_α and a_{ij}. The problem of integrating the elastoplastic equations reduces to the solution of the following set of $8 + \alpha$ non-linear equations

$$0 = \Delta E_P \frac{\partial F}{\partial \bar{Q}} + \Delta E_Q \frac{\partial F}{\partial \bar{P}} \tag{41}$$

$$0 = \Phi(\Delta E_P, \Delta E_Q, H_\beta, A_{kl}) \tag{42}$$

$$\Delta H_\alpha = \bar{h}_\alpha(\Delta E_P, \Delta E_Q, H_\beta, A_{kl}) \tag{43}$$

$$\Delta A_{ij} = \bar{a}_{ij}(\Delta E_P, \Delta E_Q, H_\beta, A_{kl}) \tag{44}$$

for the $8 + \alpha$ unknowns ΔE_P, ΔE_Q, H_α, A_{ij}. If the A_{ij} vanish the set of nonlinear equations originally derived by Aravas [3] results. A strategy, similar to that originally proposed by Aravas [3] is used here to solve the set of nonlinear equations. The variables ΔE_P and ΔE_Q are chosen as primary unknowns and (41), (42) are treated as the basic equations which are solved using Newton-Raphson method. In the following the strategy is explained more detailed using the notations

$$\Gamma_1 := \Delta E_P \frac{\partial F}{\partial \bar{Q}} + \Delta E_Q \frac{\partial F}{\partial \bar{P}} = 0 \ , \tag{45}$$

$$\Gamma_2 := \Phi(\Delta E_P, \Delta E_Q, H_\beta, A_{kl}) = 0 \ , \tag{46}$$

$$G_\alpha := \Delta H_\alpha - \bar{h}_\alpha(\Delta E_P, \Delta E_Q, H_\beta, A_{kl}) = 0 \ , \tag{47}$$

$$\Omega_{ij} := \Delta A_{ij} - \bar{a}_{ij}(\Delta E_P, \Delta E_Q, H_\beta, A_{kl}) = 0 \ . \tag{48}$$

Application of the Newton-Raphson method to (45) and (46) leads to

$$\Gamma_i + \frac{\partial \Gamma_i}{\partial \triangle E_P} \mathrm{d}\triangle E_P + \frac{\partial \Gamma_i}{\partial \triangle E_Q} \mathrm{d}\triangle E_Q + \frac{\partial \Gamma_i}{\partial A_{kl}} \mathrm{d}A_{kl} + \frac{\partial \Gamma_i}{\partial H_\alpha} \mathrm{d}H_\alpha = 0 \tag{49}$$

The $\mathrm{d}H_\alpha$ and $\mathrm{d}A_{kl}$ in (49) are derived by total differentiation of (47) and (48)

$$\frac{\partial G_\alpha}{\partial \triangle E_P} \mathrm{d}\triangle E_P + \frac{\partial G_\alpha}{\partial \triangle E_Q} \mathrm{d}\triangle E_Q + \frac{\partial G_\alpha}{\partial A_{kl}} \mathrm{d}A_{kl} + \frac{\partial G_\alpha}{\partial H_\beta} \mathrm{d}H_\beta = 0 \tag{50}$$

$$\frac{\partial \Omega_{ij}}{\partial \triangle E_P} \mathrm{d}\triangle E_P + \frac{\partial \Omega_{ij}}{\partial \triangle E_Q} \mathrm{d}\triangle E_Q + \frac{\partial \Omega_{ij}}{\partial A_{kl}} \mathrm{d}A_{kl} + \frac{\partial \Omega_{ij}}{\partial H_\beta} \mathrm{d}H_\beta = 0 \ . \tag{51}$$

From (51) follows

$$\mathrm{d}A_{ij} = \gamma_{ijmn} \left[\frac{\partial \bar{a}_{mn}}{\partial \Delta E_P} \mathrm{d}\Delta E_P + \frac{\partial \bar{a}_{mn}}{\partial \Delta E_Q} \mathrm{d}\Delta E_Q + \frac{\partial \bar{a}_{mn}}{\partial H_\beta} \mathrm{d}H_\beta \right] \tag{52}$$

with

$$\gamma_{ijkl} := \left[\frac{\partial \Omega_{ij}}{\partial A_{kl}} \right]^{-1} = \left[I_{ijkl} - \frac{\partial \bar{a}_{ij}}{\partial A_{kl}} \right]^{-1} \tag{53}$$

where the superscript (−1) indicates the inverse of the considered quantity. Introducing of (52) into (50) gives

$$\mathrm{d}H_\alpha = c_{\alpha\beta} \left[\left(\frac{\partial \bar{h}_\beta}{\partial \Delta E_P} + \frac{\partial \bar{h}_\beta}{\partial A_{ij}} \gamma_{ijkl} \frac{\partial \bar{a}_{kl}}{\partial \Delta E_P} \right) \mathrm{d}\triangle E_P + \left(\frac{\partial \bar{h}_\beta}{\partial \Delta E_Q} + \frac{\partial \bar{h}_\beta}{\partial A_{ij}} \gamma_{ijkl} \frac{\partial \bar{a}_{kl}}{\partial \Delta E_Q} \right) \mathrm{d}\triangle E_Q \right] \tag{54}$$

with

$$c_{\alpha\beta} = \left[\delta_{\alpha\beta} - \frac{\partial \bar{h}_\alpha}{\partial H_\beta} - \frac{\partial \bar{h}_\alpha}{\partial A_{kl}} \gamma_{klmn} \frac{\partial \bar{a}_{mn}}{\partial H_\beta} \right]^{-1} \ . \tag{55}$$

Introducing (54) and (52) into (49) finally leads to the reduced Newton-Raphson scheme

$$S_{11} c_P + S_{12} c_Q = B_1 \ , \tag{56}$$

$$S_{21} c_P + S_{22} c_Q = B_2 \ , \tag{57}$$

where the notations

$$c_P = \mathrm{d}\Delta E_P \tag{58}$$

$$c_Q = \mathrm{d}\Delta E_Q \tag{59}$$

are used. The constants S_{ij} and B_i are given in Appendix I. These equations are solved for c_P and c_Q, and the values of $\triangle E_P$, $\triangle E_Q$ then have to be updated:

$$\triangle E_P \rightarrow \triangle E_P + c_P \ , \tag{60}$$

$$\triangle E_Q \rightarrow \triangle E_Q + c_Q \ . \tag{61}$$

The state variables H_α and A_{ij} are updated by solving (43) for the $\triangle H_\alpha$ and (44) for the ΔA_{ij} respectively. It depends on the structure of (43) and (44) whether the H_α and A_{ij} can be updated by solving simple linear equations or if a system of nonlinear equations has to be solved. The values for $\bar{P}$ and $\bar{Q}$ then can be updated using the Eqs. (37) and (38). This iterative loop has to be continued until convergence for ΔE_P and ΔE_Q is achieved.

4.2
Calculation of the consistent tangent matrix

If an implicit integration method is used, a so-called consistent material tangent has to be calculated to ensure quadratic convergence of the global equilibrium iteration. From (27) and (32) follows

$$\Delta\Sigma_{ij} = C_{ijkl} \left(\Delta E_{kl} - \tfrac{1}{3} \Delta E_P \delta_{kl} - \bar{N}_{kl} \Delta E_Q \right) \ . \tag{62}$$

Total differentiation of (62) gives

$$\mathrm{d}\Delta\Sigma_{ij} = C_{ijkl} \left(\mathrm{d}\Delta E_{kl} - \tfrac{1}{3} \delta_{kl} \mathrm{d}\Delta E_P - \bar{N}_{kl} \mathrm{d}\Delta E_Q - \Delta E_Q J_{klmn} \left[\mathrm{d}A_{mn} + \mathrm{d}\Sigma^{\mathrm{pred}}_{mn} \right] \right) \tag{63}$$

with

$$J_{klmn} = \tfrac{1}{\theta} \left(\tfrac{3}{2} I_{klmn} - \tfrac{1}{2} \delta_{kl} \delta_{mn} - \bar{N}_{kl} \bar{N}_{mn} \right) \tag{64}$$

where $\theta = \bar{Q} + 3G\Delta E_Q$ and

$$J_{klmn} = \frac{\partial \bar{N}_{kl}}{\partial \Sigma^{\mathrm{pred}}_{mn}} = -\frac{\partial \bar{N}_{kl}}{\partial A_{mn}} \ . \tag{65}$$

The $\mathrm{d}\Delta E_P$, $\mathrm{d}\Delta E_Q$ and $\mathrm{d}A_{kl}$ in (63) now have to be expressed in terms of $\mathrm{d}\Sigma^{\mathrm{pred}}_{mn}$. Total differentiation of (43) and (44) gives after some algebraic calculations

$$\mathrm{d}H_\alpha = \frac{\partial H_\alpha}{\partial \Delta E_P} \mathrm{d}\Delta E_P + \frac{\partial H_\alpha}{\partial \Delta E_Q} \mathrm{d}\Delta E_Q + \frac{\partial H_\alpha}{\partial \Sigma^{\mathrm{pred}}_{mn}} \mathrm{d}\Sigma^{\mathrm{pred}}_{mn} \tag{66}$$

$$\mathrm{d}A_{kl} = \frac{\partial A_{kl}}{\partial \Delta E_P} \mathrm{d}\Delta E_P + \frac{\partial A_{kl}}{\partial \Delta E_Q} \mathrm{d}\Delta E_Q + \frac{\partial A_{kl}}{\partial \Sigma^{\mathrm{pred}}_{mn}} \mathrm{d}\Sigma^{\mathrm{pred}}_{mn} \tag{67}$$

where the $\partial H_\alpha/\partial \Delta E_P$, $\partial H_\alpha/\partial \Delta E_Q$, $\partial A_{kl}/\partial \Delta E_P$, $\partial A_{kl}/\partial \Delta E_Q$ are given in Appendix I and the $\partial H_\alpha/\partial \Delta\Sigma^{\mathrm{pred}}_{mn}$, $\partial A_{kl}/\partial \Sigma^{\mathrm{pred}}_{mn}$ are given in Appendix II. Total differentiation of (41) and (42) leads to

$$\begin{aligned}
&\frac{\partial F}{\partial \bar{Q}} \mathrm{d}E_P + \frac{\partial F}{\partial \bar{P}} \mathrm{d}E_Q + \Delta E_P \Bigg[\left(-\frac{1}{3} \frac{\partial^2 F}{\partial \bar{Q} \partial \bar{P}} \delta_{mn} + \frac{\partial^2 F}{\partial \bar{Q}^2} \bar{N}_{mn} \right) \mathrm{d}\Sigma^{\mathrm{pred}}_{mn} \\
&\quad + \left(\frac{1}{3} \frac{\partial^2 F}{\partial \bar{Q} \partial \bar{P}} \delta_{kl} - \frac{\partial^2 F}{\partial \bar{Q}^2} \bar{N}_{kl} \right) \mathrm{d}A_{kl} + \frac{\partial^2 F}{\partial \bar{Q} \partial H_\alpha} \mathrm{d}H_\alpha \Bigg] \\
&\quad + \Delta E_Q \Bigg[\left(-\frac{1}{3} \frac{\partial^2 F}{\partial \bar{P}^2} \delta_{mn} + \frac{\partial^2 F}{\partial \bar{P} \partial \bar{Q}} \bar{N}_{mn} \right) \mathrm{d}\Sigma^{\mathrm{pred}}_{mn} \\
&\quad + \left(\frac{1}{3} \frac{\partial^2 F}{\partial \bar{P}^2} \delta_{kl} - \frac{\partial^2 F}{\partial \bar{P} \partial \bar{Q}} \bar{N}_{kl} \right) \mathrm{d}A_{kl} \\
&\quad + \frac{\partial^2 F}{\partial \bar{P} \partial H_\alpha} \mathrm{d}H_\alpha \Bigg] = 0
\end{aligned} \tag{68}$$

and

$$\left(-\frac{1}{3}\frac{\partial\Phi}{\partial\bar{P}}\delta_{mn}+\frac{\partial\Phi}{\partial\bar{Q}}\bar{N}_{mn}\right)\mathrm{d}\Sigma^{\mathrm{pred}}_{mn}+\frac{\partial\Phi}{\partial H_\alpha}\mathrm{d}H_\alpha + \left(\frac{1}{3}\frac{\partial\Phi}{\partial\bar{P}}\delta_{kl}-\frac{\partial\Phi}{\partial\bar{Q}}\bar{N}_{kl}\right)\mathrm{d}A_{kl}=0\ , \quad (69)$$

respectively. Introducing (66) and (67) into (68) and (69) leads to the following system of linear equations

$$S_{11}\mathrm{d}\Delta E_P+S_{12}\mathrm{d}\Delta E_Q=B^{(1)}_{mn}\mathrm{d}\Sigma^{\mathrm{pred}}_{mn} \quad (70)$$

$$S_{21}\mathrm{d}\Delta E_P+S_{22}\mathrm{d}\Delta E_Q=B^{(2)}_{mn}\mathrm{d}\Sigma^{\mathrm{pred}}_{mn} \quad (71)$$

where the constants S_{ij} are exactly the same as in (56) and (57). $B^{(1)}_{mn}$, $B^{(2)}_{mn}$ can be found in Appendix II. The linear system (70), (71) can be solved to get the following representation of $\mathrm{d}\Delta E_P$ and $\mathrm{d}\Delta E_Q$

$$\mathrm{d}\Delta E_P=B^{(P)}_{mn}\mathrm{d}\Sigma^{\mathrm{pred}}_{mn} \quad (72)$$

$$\mathrm{d}\Delta E_Q=B^{(Q)}_{mn}\mathrm{d}\Sigma^{\mathrm{pred}}_{mn} \quad (73)$$

which can be done for example by applying Cramer's rule. Using (72), (73), (67), Eq. (62) can be written as

$$\mathrm{d}\Sigma_{ij}=C_{ijkl}\left(\mathrm{d}E_{kl}-M_{klmn}\mathrm{d}\Sigma^{\mathrm{pred}}_{mn}\right) \quad (74)$$

with

$$M_{klmn}=+\tfrac{1}{3}\delta_{mn}B^{(P)}_{mn}+\bar{N}_{kl}B^{(Q)}_{mn} - J_{klop}\left(\frac{\partial A_{op}}{\partial\Delta E_P}B^{(P)}_{mn}+\frac{\partial A_{op}}{\partial\Delta E_Q}B^{(Q)}_{mn}\right) + \Delta E_Q\left(J_{klmn}-J_{klop}\frac{\partial A_{op}}{\partial\Sigma^{\mathrm{pred}}_{mn}}\right) \quad (75)$$

where J_{ijkl} has been already defined by Eq. (64). Finally, from (34) follows

$$\mathrm{d}\Sigma^{\mathrm{pred}}_{ij}=C_{ijkl}\mathrm{d}\Delta E_{kl} \quad (76)$$

which together with (74) leads to

$$\mathrm{d}\Delta\Sigma_{ij}=\left(C_{ijkl}-C_{ijop}M_{opmn}C_{mnkl}\right)\mathrm{d}\Delta E_{kl} \quad (77)$$

and means that the consistent tangent D_{ijkl} is explicitly given by

$$D_{ijkl}=C_{ijkl}-C_{ijop}M_{opmn}C_{mnkl} \quad (78)$$

5
Gurson-type constitutive equations including kinematic hardening

Considering a material whose microstructure is characterized by the existence of voids and/or particles which may cause void nucleation, a ductile damage model was proposed by Gurson [8]. The model incorporates void growth, void nucleation and coalescence of voids and has been modified by various authors. The modifications which are significant for the work presented here will be discussed next. Here, the Gurson-type yield function

$$\Phi=\left(\frac{\bar{Q}}{\Sigma_1}\right)^2+2q_1f^*\ \cosh\left(-\frac{3}{2}q_2\frac{\bar{P}}{\Sigma_2}\right)-1-q_3(f^*)^2 \quad (79)$$

is used. The fit parameters q_1, q_2, q_3 in (79) have been introduced by Tvergaard [9] into the model, originally proposed by Gurson [8] to get a better agreement between the predictions of the Gurson model with the results obtained by cell model calculations. To take into account the loss of stress carrying capacity associated with void coalescence, Tvergaard and Needleman [10] proposed the modified damage parameter f^* as a piecewise linear function of the void volume fraction f

$$f^*=\begin{cases} f & f\le f_c \\ f_c+\kappa(f-f_c) & f>f_c \end{cases} \quad \text{with } \kappa=\frac{f^*_U-f_c}{f_F-f_c}\ . \quad (80)$$

The parameter f^*_U is related to q_1 by $f^*_U=1/q_1$ if $q_3=q_1^2$ is used. The void volume fraction where void coalescence starts is indicated by f_c and the void volume fraction at final fracture is denoted by f_F.

Usually, Σ_1 and Σ_2 in (79) are identified with a single parameter, the yield stress σ_{Y_0} in the case of an ideal plastic matrix material, or with an averaged yield stress σ_Y related to some averaged equivalent strain $\bar{\varepsilon}$ through the hardening law of the matrix material. For this case Leblond et al. [11] discovered incompatibilities of the predictions made by the Gurson-model with the analytical solution for a hollow sphere in a rigid hardening matrix material in hydrostatic tension. Furthermore, if a single parameter is used for Σ_1 and Σ_2, the progressive increase of f which can be observed under cyclic loading using cell model calculations (see [12]) cannot be reproduced by the Gurson-model. To avoid the discrepancies mentioned above, Leblond et al. [11] performed a homogenization of the boundary value problem of a sperical void in a hardening matrix and derived the expressions

$$\Sigma_1=\frac{1}{b^3-a^3}\int_{a^3}^{b^3}\sigma_Y(\langle\bar{\varepsilon}\rangle_{r^3})\mathrm{d}r^3 \quad (81)$$

$$\Sigma_2=\frac{1}{\ln(b^3/a^3)}\int_{a^3}^{b^3}\sigma_Y(\langle\bar{\varepsilon}\rangle_{r^3})\frac{\mathrm{d}r^3}{r^3}\ . \quad (82)$$

with

$$\langle\bar{\varepsilon}\rangle_{r^3}=\frac{2}{3}\left[\sinh^{-1}u-\frac{\sqrt{1+u^2}}{u}\right]_{u_1=2E_H/(E_{\mathrm{eqv}}r^3)}^{u_2=2E_H/(E_{\mathrm{eqv}}\rho^3)} \quad (83)$$

and

$$a^3=\exp(3E_H)-1+f_0 \quad (84)$$

$$b^3=\exp(3E_H) \quad (85)$$

$$\rho^3=r^3-b^3+1 \quad (86)$$

$$E_H=\int_0^t\frac{|\dot{E}_P|}{3}\mathrm{d}\tau \quad (87)$$

$$E_{\mathrm{eqv}}=\int_0^t|\dot{E}_Q|\mathrm{d}\tau \quad (88)$$

where f_0 denotes the initial void volume fraction. As one can see from (83), $\bar{\varepsilon}$ is fully determined by the E^{pl}_{ij} so that within the model used here $\bar{\varepsilon}$ is no internal variable like for example within the Gurson-type model used in [13]. Here, the only internal variable of the type of H_α is the void volume fraction f. The change in void volume fraction arises partly from growth of existing voids and partly from nucleation of new voids:

$$\dot{f} = \dot{f}_{\text{growth}} + \dot{f}_{\text{nucleation}} \quad . \tag{89}$$

From incompressible matrix behaviour follows

$$\dot{f}_{\text{growth}} = (1-f)\dot{E}_P \quad . \tag{90}$$

Void nucleation based on plastic straining is included so that

$$\dot{f}_{\text{nucleation}} = \mathcal{A}\dot{\bar{E}} \quad . \tag{91}$$

The quantity $\mathcal{A}$ derives from a normal distribution as suggested in [13]

$$\mathcal{A} = \frac{f_N}{s_N\sqrt{2\pi}} \exp\left(-\frac{1}{2}\left[\frac{\bar{E}-\epsilon_N}{s_N}\right]^2\right) \tag{92}$$

with

$$\bar{E} = \frac{1}{b^3-a^3}\int_{a^3}^{b^3} \langle\bar{\varepsilon}\rangle_{r^3} \mathrm{d}r^3 = \frac{1}{1-f_0}\int_{a^3}^{b^3} \langle\bar{\varepsilon}\rangle_{r^3} \mathrm{d}r^3 \tag{93}$$

The equation for $\mathcal{A}$ is based on the assumption that the nucleation strain follows a normal distribution arround ϵ_N with the standard deviation s_N. The volume fraction of nucleating particles f_N has to be determined so that f_N is consistent with the void volume fraction of particles.

If a material point loses its stress carrying capacity, the stresses Σ_{ij} have to vanish. This is only possible if the backstresses A_{ij} vanish, too. Therefore, following [14], the backstresses A_{ij} are written as

$$A_{ij} = g(f^*)A^*_{ij} \tag{94}$$

where

$$g(f^*) = 1 - f^*/f^*_U \quad . \tag{95}$$

The following evolution equations

$$\overset{\triangledown}{A}{}^*_{ij} = \left(C\frac{1}{\Sigma_1}S_{ij} - \bar{\gamma}A_{ij}\right)\dot{\bar{E}} \tag{96}$$

have been chosen for the A^*_{ij}. The Eqs. (96) are similar to the evolution equations proposed by Lemaitre and Chaboche [15] for the case of classical isothermal plasticity including linear and nonlinear kinematic hardening and available in the finite element program Abaqus.

C and $\bar{\gamma}$ in (96) are material parameters related to linear and nonlinear hardening, respectively. The use of (96) allows a quite easy verification of the integration algorithm on the basis of special cases.

Derivation of (94) according to (8) leads to

$$\overset{\triangledown}{A}_{ij} = \frac{\dot{g}}{g}A_{ij} + \overset{\triangledown}{A}{}^*_{ij} \quad . \tag{97}$$

In the following, the backward Euler method (29) is applied to the Gurson-type model considered here. Equations (41) and (42) given in Sect. 4 can be used without further specifications. Application of the Euler scheme to (89) leads to

$$\Delta f = (1-f)\Delta E_P + \mathcal{A}\Delta\bar{E} \tag{98}$$

and with respect to (97)

$$\Delta A_{ij} = d_1\left[\frac{C}{\Sigma_1}\left(\Sigma^{\text{pred}}_{ij} - K\Delta E_P\delta_{ij} - 2G\Delta E_Q\bar{N}_{ij}\right) - {}^tA_{ij}\left(\frac{C}{\Sigma_1}+\bar{\gamma}\right)\right] - d_2\,{}^tA_{ij} \tag{99}$$

was obtained, where

$$d_1 = \frac{\Delta E}{\frac{f^*_U - {}^tf^*}{f^*_U - f^*} + \left(\frac{C}{\Sigma_1}+\bar{\gamma}\right)\Delta E} \tag{100}$$

$$d_2 = \frac{\Delta f^*}{\frac{f^*_U - {}^tf^*}{f^*_U - f^*} + \left(\frac{C}{\Sigma_1}+\bar{\gamma}\right)\Delta E} \quad . \tag{101}$$

To obtain (99), the Eqs. (33), (94), (95) were used and the relation $A_{ij} = {}^tA_{ij} + \Delta A_{ij}$ was applied. Finally, the necessary equations are (41), (42), (98) and (99). $\bar{P}$ and $\bar{Q}$ in (41) and (42) are already given by (37) and (38), respectively. The identities $\Delta A_{ij} = \bar{a}_{ij}$ and $\Delta f = \bar{h}$ hold with respect to the integration scheme developed in general in Sect. 4 . The Σ_1, Σ_2, $\bar{E}$, $\mathcal{A}(\bar{E})$ finally depend only on the strain variables E_H and E_{eqv} which can be written as

$$E_H = {}^tE_H + \frac{|\Delta E_P|}{3} \tag{102}$$

$$E_{\text{eqv}} = {}^tE_{\text{eqv}} + |\Delta E_Q| \quad . \tag{103}$$

It is worth noting that due to the symmetry of Σ the following symmetries

$$\bar{a}_{ij} = \bar{a}_{ji} \tag{104}$$

$$A_{ij} = A_{ji} \tag{105}$$

$$\frac{\partial\bar{a}_{ij}}{\partial A_{kl}} = \frac{\partial\bar{a}_{ji}}{\partial A_{kl}} = \frac{\partial\bar{a}_{ij}}{\partial A_{lk}} \quad , \tag{106}$$

are valid. Furthermore, the inversion included in (53) to obtain the fourth order tensor γ_{ijkl} can be performed analytically for the Gurson-type model which gives

$$\gamma_{ijkl} = \frac{2\Theta}{2(\bar{Q}+3G\Delta E_Q)+3\Theta}\left(\frac{1}{2}\delta_{ij}\delta_{kl} + \bar{N}_{ij}\bar{N}_{kl}\right) + \frac{2(\bar{Q}+3G\Delta E_Q)+3\Theta}{2(\bar{Q}+3G\Delta E_Q)}I_{ijkl} \tag{107}$$

where Θ is given by

$$\Theta = -2G\Delta E_Q\frac{C\Delta E_Q}{\Sigma_1 + C\Delta E_Q} \quad . \tag{108}$$

The Gurson-type model has been implemented in the way described above into the finite element program Abaqus [4].

6
Numerical examples

6.1
General remarks and definitions

The predictions of the Gurson-like model described in the previous section have been compared with the results of cell model calculations. Cylindrical unit cells with a spherical void in the centre surrounded by an elastic-plastic matrix material are considered. To avoid a possible confusion with the overall quantities Σ_{ij} and A_{ij} of the Gurson-type model, the stresses and the backstresses inside the matrix are denoted by σ_{ij} and α_{ij}, respectively. Mixed nonlinear hardening of the matrix material has been considered and constitutive equations of classical elasto-plasticity including isotropic and kinematic hardening were used. The elasto-plastic regime is characterized by the yield condition

$$\varphi = \sqrt{\tfrac{3}{2}\left(\sigma'_{ij} - \alpha'_{ij}\right)\left(\sigma'_{ij} - \alpha'_{ij}\right)} - \sigma_Y(\bar{\varepsilon}) \tag{109}$$

where isotropic hardening is controlled by $\sigma_Y(\bar{\varepsilon})$ and kinematic hardening by the backstresses a_{ij}. The accumulated equivalent plastic strain $\bar{\varepsilon}$ is given as

$$\bar{\varepsilon} = \int_0^t \sqrt{\frac{2}{3}\dot{\varepsilon}^{\mathrm{pl}}_{kl}\dot{\varepsilon}^{\mathrm{pl}}_{kl}}\,\mathrm{d}\tau \ . \tag{110}$$

The $\dot{\varepsilon}^{\mathrm{pl}}_{kl}$ in (110) denote the components of the plastic strain rate tensor and t denotes a loading parameter or time, respectively. The evolution of the backstresses is described by the Chaboche-model [15]

$$\overset{\triangledown}{\alpha}_{ij} = \left[\frac{C^M}{\sigma_Y(\bar{\varepsilon})}\left(\sigma_{ij} - \alpha_{ij}\right) - \bar{\gamma}^M \alpha_{ij}\right]\dot{\bar{\varepsilon}} \tag{111}$$

which consists of the Ziegler-law to describe linear kinematic hardening controlled by the parameter C^M and the so-called recall term to introduce nonlinear kinematic hardening. In order to point out clearly that these properties are properties of the matrix material, the superscript M is used here. Isotropic hardening of the matrix material is given by

$$\sigma_Y(\bar{\varepsilon}) = \sigma_{Y_0} + Q_\infty\left[1 - \exp\left(-b^M\bar{\varepsilon}\right)\right] \tag{112}$$

with $\sigma_{Y_0} = 200$ MPa, $Q_\infty = 294.1$ MPa and $b^M = 34$. Furthermore, an initial void volume fraction $f_0 = 0.01$ was chosen. The geometry of the cylindrical cell and the finite element mesh which is a quarter section due to the symmetry conditions are shown in Fig. 1. The notations used in the following to explain the geometrical dimensions, the boundary conditions and the applied loading can also be found in Fig. 1. The initial diameter and height of the cell, R and H, are $R(t=0) = H(t=0) = R_0$. The symmetry conditions are imposed as boundary conditions

$$u_2(x_2 = 0, x_3) = 0 \tag{113}$$

$$u_3(x_3 = 0, x_2) = 0 \ . \tag{114}$$

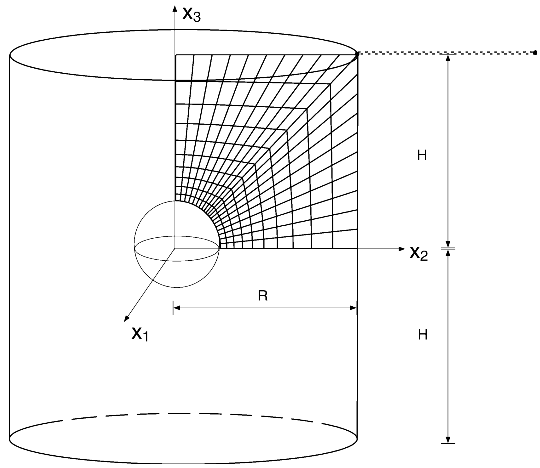

Fig. 1. Initial geometry and finite element mesh

To ensure periodicity of the cell arrangement, the further boundary conditions

$$u_2(x_2 = R, x_3 \in (0, H)) = \bar{u}_2 \tag{115}$$

$$u_3(x_2 \in (0, R), x_3 = H) = \bar{u}_3 \tag{116}$$

are introduced.

The overall Cauchy stress tensor Σ and the tensor of the overall total logarithmic strains $\mathbf{E}^{(\log)}$ which correspond to the applied loading are qualitatively given by

$$\Sigma = \begin{pmatrix} \Sigma_{11} & 0 & 0 \\ 0 & \Sigma_{11} & 0 \\ 0 & 0 & \Sigma_{33} \end{pmatrix} \mathbf{e_i} \otimes \mathbf{e_j} \ , \tag{117}$$

$$\mathbf{E}^{(\log)} = \begin{pmatrix} E^{(\log)}_{11} & 0 & 0 \\ 0 & E^{(\log)}_{11} & 0 \\ 0 & 0 & E^{(\log)}_{33} \end{pmatrix} \mathbf{e}_i \otimes \mathbf{e}_j \tag{118}$$

where the components of the overall Cauchy stress tensor were calculated by the sum of the corresponding reaction forces on the outer boundary of the unit cell divided by the actual area. The overall logarithmic strains are given as

$$E^{(\log)}_{11} = E^{(log)}_{22} = \ln\left(1 + \frac{\bar{u}_2}{R_0}\right) \tag{119}$$

$$E^{(\log)}_{33} = \ln\left(1 + \frac{\bar{u}_3}{R_0}\right) \ . \tag{120}$$

The overall von Mises equivalent stress and the overall equivalent total strain are

$$\Sigma_{\mathrm{eqv}} = \left|\Sigma_{33} - \Sigma_{11}\right| \tag{121}$$

$$E_{\mathrm{eqv}} = \tfrac{2}{3}\left|E_{33} - E_{11}\right| \tag{122}$$

The overall stress triaxiality T is defined by

$$T = \frac{\Sigma_{\mathrm{hyd}}}{\Sigma_{\mathrm{eqv}}} \tag{123}$$

where Σ_{hyd} stands for the overall hydrostatic stress

$$\Sigma_H = \tfrac{1}{3}\left(2\Sigma_{11} + \Sigma_{33}\right) \ . \tag{124}$$

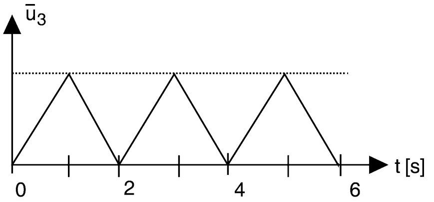

Fig. 2. Displacement $\bar{u}_3$ applied in the case of cyclic loading

Here, instead of (121) and (122), the signed quantities

$$\Sigma^* = (\Sigma_{33} - \Sigma_{11}) \quad (125)$$

$$E^* = 2/3(E_{33} - E_{11}) \quad (126)$$

are used to discuss the results. The calculations have been carried out at constant overall stress triaxialities. The displacement $\bar{u}_3$ has been prescribed as function of time or loading parameter, respectively, which is shown in Fig. 2, and a linear elastic truss parallel to the x_2 axis has been used which is drawn schematically as a dashed line in Fig. 1. Constant overall stress triaxiality has been ensured by adapting the stiffness of the truss during the calculations. A maximum value of $0.05R_0$ has been chosen for $\bar{u}_3$. The same kinematic hardening parameters were taken for the matrix material and the Gurson-type material, i.e. $C^M = C$ and $\bar{\gamma}^M = \bar{\gamma}$.

6.2 Results and discussion

The results obtained by cell model calculations for the overall stress triaxialities $T = 1$, $T = 2$ and $T = 3$ are presented together with the corresponding predictions of the Gurson-type model in Fig. 3. From these results it is deduced that the Gurson-type model overestimates in general the evolution of the void volume fraction f. The results obtained by the cell model calculations show a ratcheting effect with respect to f. This effect increases with increasing overall stress triaxiality. The Gurson-type model predicts the ratcheting qualitatively in the same way but it predicts the effect quantitatively much weaker. However, the $\Sigma^*(E^*)$-curves of the Gurson-type model are very close to the corresponding curves obtained by cell model calculations and the lower the overall stress triaxiality the better the agreement between the Gurson-type model and cell model calculations.

7 Concluding remarks

To integrate implicitely a class of constitutive equations of elastoplasticity including pressure dependent yield condition and flow rule, isotropic hardening and damage, an algorithm has been proposed by Aravas [3]. This algorithm has been extended with respect to kinematic hardening. Like in the case of isotropic hardening the number of primary unknown involved in the Newton-Raphson iteration to solve the system of nonlinear equations can be reduced to two strain variables. Whether this algorithm is more efficient than other implicit integration schemes also based on a predictor-corrector method depends on the structure of the incremental form of the evolution equations for the internal variables. Once the two primary strain variables are known the internal variables can be

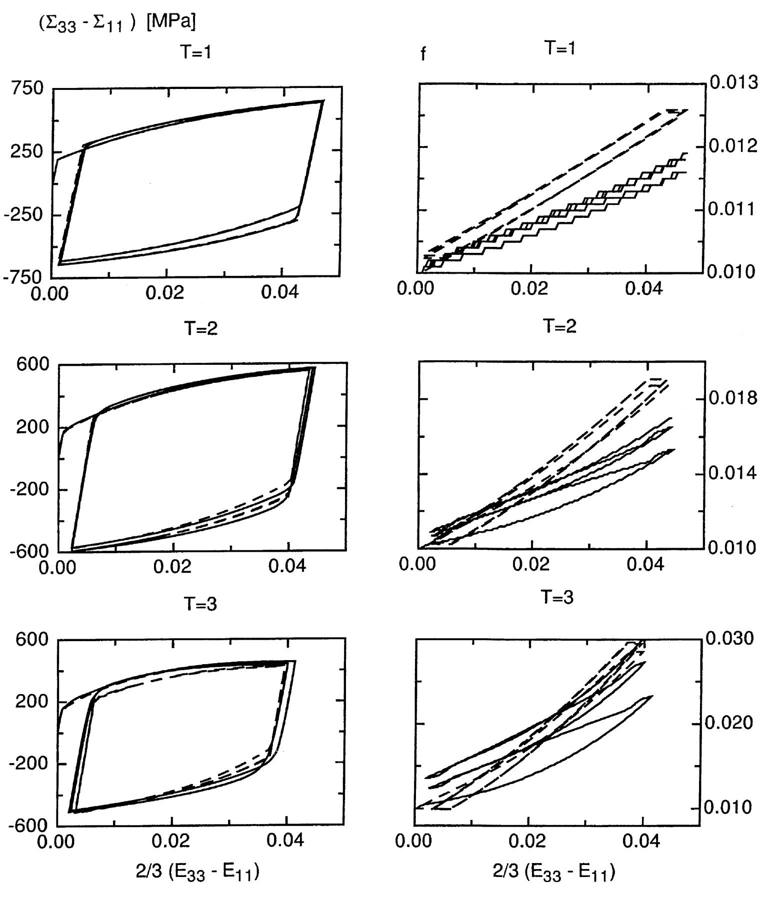

Fig. 3. Comparision of the results obtained by unit cell calculations (full lines) and by the use of the Gurson-like model (dashed lines) for cyclic loading for the material NLH_{mix} at the stress triaxialities $T = 1$, $T = 2$ and $T = 3$

updated. If the incremental evolution equations are highly nonlinear a second system of nonlinear equations has to be solved numerically. In this case the main advantage of the algorithm gets lost.

The modified Aravas-algorithm was applied to a Gurson-type model which includes kinematic hardening. The predictions of the Gurson-type model have been compared with the results obtained by cell model calculations at constant overall stress triaxialities under cyclic loading. Mixed nonlinear hardening was considered. It has been shown that the main features of ductile damage with kinematic hardening matrix material can be described. However, the model overestimates the evolution of the void volume fraction f under cyclic loading which may be caused by the fact that only the part of the modification proposed by Perrin et al. [11] related to isotropic hardening is used here.

References

1. **Simo JC, Taylor RL** (1985) Consistent tangent operators for rate-independent elastoplasticity. Comput. Meth. Appl. Mech. Eng. 48: 101–118
2. **Hartmann S, Lührs G, Haupt P** (1997) An efficient stress algorithm with applications in viscoplasticity and plasticity. Int. J. Numer. Meth. Eng. 40: 991–1013
3. **Aravas N** (1987) On the numerical integration of a class of pressure-dependent plasticity models. Int. J. Numer. Meth. Eng. 24: 1395–1416
4. **Hibbit, Karlsson & Sorensen, Inc.** (1998) ABAQUS manuals Version 5.8
5. **Hughes TJR, Winget J** (1980) Finite rotation effects in numerical integration of rate constitutive equations arising in large deformation analysis. Int. J. Numer. Meth. Eng. 15: 1862–1867
6. **Diegele E, Jansohn W, Tsakmakis Ch** (2000) Finite deformation plasticity and viscoplasticity laws exhibiting nonlinear hardening rules. Comput. Mech. 25: 1–12
7. **Svendson B, Arndt S, Klingbeil D, Sievert R** (1998) Hyperelastic models for elastoplasticity with non-linear isotropic and kinematic hardening at large deformations. Int. J. Solids Struct. 35: 3363–3389
8. **Gurson AL** (1977) Continuum theory of ductile rupture by void nucleation and growth: part I – yield criteria and flow rules for porous ductile media. J. Eng. Mater. Technol. 99: 2–15
9. **Tvergaard V** (1981) Influence of voids on shear band instabilities under plane strain conditions. Int. J. Fract. 17: 389–407
10. **Tvergaard V, Needleman A** (1984) Analysis of the cup-cone fracture in a round tensile bar. Acta Metall. 32: 157–169
11. **Leblond JB, Perrin G, Devaux J** (1995) An improved Gurson-type model for hardenable ductile metals. European J. Mech. A 14: 499–528
12. **Devaux J, Gologanu M, Leblond JB, Perrin G** (1995) On continued void growth in ductile metals subjected to cyclic loadings. In: Willis J (ed.), IUTAM Symposium on Nonlinear Analysis of Fracture. Kluwer Academic Publishers
13. **Chu CC, Needleman A** (1980) Void nucleation effects in biaxially streched sheets. J. Eng. Mater. Technol. 102: 249–256
14. **Arndt S** (2000) Modellierung der Warmvorbelastung mit einem Schädigungsmodell für kombinierte Verfestigung am Beispiel des Werkstoffs 10MnMoNi5-5 Universität Magdeburg, Diss.
15. **Lemaitre J, Chaboche JL** (1990) Mechanics of Solid Materials, Cambridge University Press

Appendix I

The constants involved in the solution of the elastoplastic equations are given by

$$S_{11} = \frac{\partial F}{\partial \bar{Q}} + \Delta E_P \left(K \frac{\partial^2 F}{\partial \bar{Q} \partial \bar{P}} + \frac{\partial^2 F}{\partial \bar{Q} \partial H_\alpha} \frac{\partial H_\alpha}{\partial \Delta E_P} + \left[\frac{\partial^2 F}{\partial \bar{Q}^2} \frac{\partial \bar{Q}}{\partial A_{ij}} + \frac{\partial^2 F}{\partial \bar{Q} \partial \bar{P}} \frac{\partial \bar{P}}{\partial A_{ij}} \right] \frac{\partial A_{ij}}{\partial \Delta E_P} \right) + \Delta E_Q \left(K \frac{\partial^2 F}{\partial \bar{P}^2} + \frac{\partial^2 F}{\partial \bar{P} \partial H_\alpha} \frac{\partial H_\alpha}{\partial \Delta E_P} + \left[\frac{\partial^2 F}{\partial \bar{Q} \partial \bar{P}} \frac{\partial \bar{Q}}{\partial A_{ij}} + \frac{\partial^2 F}{\partial \bar{P}^2} \frac{\partial \bar{P}}{\partial A_{ij}} \right] \frac{\partial A_{ij}}{\partial \Delta E_P} \right) \tag{127}$$

$$S_{12} = \frac{\partial F}{\partial \bar{P}} + \Delta E_P \left(-3G \frac{\partial^2 F}{\partial \bar{Q}^2} + \frac{\partial^2 F}{\partial \bar{Q} \partial H_\alpha} \frac{\partial H_\alpha}{\partial \Delta E_Q} + \left[\frac{\partial^2 F}{\partial \bar{Q}^2} \frac{\partial \bar{Q}}{\partial A_{ij}} + \frac{\partial^2 F}{\partial \bar{Q} \partial \bar{P}} \frac{\partial \bar{P}}{\partial A_{ij}} \right] \frac{\partial A_{ij}}{\partial \Delta E_Q} \right) + \Delta E_Q \left(-3G \frac{\partial^2 F}{\partial \bar{Q} \partial \bar{P}} + \frac{\partial^2 F}{\partial \bar{P} \partial H_\alpha} \frac{\partial H_\alpha}{\partial \Delta E_Q} + \left[\frac{\partial^2 F}{\partial \bar{Q} \partial \bar{P}} \frac{\partial \bar{Q}}{\partial A_{ij}} + \frac{\partial^2 F}{\partial \bar{P}^2} \frac{\partial \bar{P}}{\partial A_{ij}} \right] \frac{\partial A_{ij}}{\partial \Delta E_Q} \right) \tag{128}$$

$$S_{21} = K \frac{\partial \Phi}{\partial \bar{P}} + \frac{\partial \Phi}{\partial H_\alpha} \frac{\partial H_\alpha}{\partial \Delta E_P} + \left[\frac{\partial \Phi}{\partial \bar{P}} \frac{\partial \bar{P}}{\partial A_{ij}} + \frac{\partial \Phi}{\partial \bar{Q}} \frac{\partial \bar{Q}}{\partial A_{ij}} \right] \frac{\partial A_{ij}}{\partial \Delta E_P} \tag{129}$$

$$S_{22} = -3G \frac{\partial \Phi}{\partial \bar{Q}} + \frac{\partial \Phi}{\partial H_\alpha} \frac{\partial H_\alpha}{\partial \Delta E_Q} + \left[\frac{\partial \Phi}{\partial \bar{P}} \frac{\partial \bar{P}}{\partial A_{ij}} + \frac{\partial \Phi}{\partial \bar{Q}} \frac{\partial \bar{Q}}{\partial A_{ij}} \right] \frac{\partial A_{ij}}{\partial \Delta E_Q} \tag{130}$$

and

$$B_1 = -\Delta E_P \frac{\partial F}{\partial \bar{Q}} - \Delta E_Q \frac{\partial F}{\partial \bar{P}} \tag{131}$$

$$B_2 = -\Phi \tag{132}$$

where

$$\frac{\partial H_\alpha}{\partial \Delta E_P} = c_{\alpha\beta} \left[\frac{\partial \bar{h}_\beta}{\partial \Delta E_P} + \frac{\partial \bar{h}_\beta}{\partial A_{ij}} \gamma_{ijkl} \frac{\partial \bar{a}_{kl}}{\partial \Delta E_P} \right] \tag{133}$$

$$\frac{\partial H_\alpha}{\partial \Delta E_Q} = c_{\alpha\beta} \left[\frac{\partial \bar{h}_\beta}{\partial \Delta E_Q} + \frac{\partial \bar{h}_\beta}{\partial A_{ij}} \gamma_{ijkl} \frac{\partial \bar{a}_{kl}}{\partial \Delta E_Q} \right] \tag{134}$$

$$\frac{\partial A_{ij}}{\partial \Delta E_P} = \gamma_{ijmn} \left[\frac{\partial \bar{a}_{mn}}{\partial \Delta E_P} + \frac{\partial \bar{a}_{mn}}{\partial H_\beta} \frac{\partial H_\beta}{\partial \Delta E_P} \right] \tag{135}$$

$$\frac{\partial A_{ij}}{\partial \Delta E_Q} = \gamma_{ijmn} \left[\frac{\partial \bar{a}_{mn}}{\partial \Delta E_Q} + \frac{\partial \bar{a}_{mn}}{\partial H_\beta} \frac{\partial H_\beta}{\partial \Delta E_Q} \right] \tag{136}$$

with

$$\gamma_{ijkl} = \left[I_{ijkl} - \frac{\partial \bar{a}_{ij}}{\partial A_{kl}} \right]^{-1} \tag{137}$$

$$c_{\alpha\beta} = \left[\delta_{\alpha\beta} - \frac{\partial \bar{h}_{\alpha}}{\partial H_{\beta}} - \frac{\partial \bar{h}_{\alpha}}{\partial A_{kl}} \gamma_{klmn} \frac{\partial \bar{a}_{mn}}{\partial H_{\beta}} \right]^{-1} . \tag{138}$$

Appendix II

The $B^{(1)}_{mm}$ and $B^{(2)}_{mm}$ which are involved into the calculation of the consistent tangent matrix are given by

$$B^{(1)}_{mm} = \frac{1}{3} \Delta E_Q \frac{\partial^2 F}{\partial \bar{P}^2} \left(\delta_{mn} - \delta_{op} \frac{\partial A_{op}}{\partial \Sigma^{\text{pred}}_{mn}} \right) - \Delta E_P \frac{\partial^2 F}{\partial \bar{Q}^2} \left(\bar{N}_{mn} - \bar{N}_{op} \frac{\partial A_{op}}{\partial \Sigma^{\text{pred}}_{mn}} \right) \tag{139}$$

$$B^{(2)}_{mm} = \frac{1}{3} \frac{\partial \Phi}{\partial \bar{P}} \left(\delta_{mn} - \delta_{op} \frac{\partial A_{op}}{\partial \Sigma^{\text{pred}}_{mn}} \right) - \frac{\partial \Phi}{\partial \bar{Q}} \left(\bar{N}_{mn} - \bar{N}_{op} \frac{\partial A_{op}}{\partial \Sigma^{\text{pred}}_{mn}} \right) \tag{140}$$

where

$$\frac{\partial H_{\alpha}}{\partial \Sigma^{\text{pred}}_{mn}} = c_{\alpha\beta} \left(\frac{\partial \bar{h}_{\beta}}{\partial \Sigma^{\text{pred}}_{mn}} + \frac{\partial \bar{h}_{\beta}}{\partial A_{kl}} \gamma_{klop} \frac{\partial \bar{a}_{op}}{\partial \Sigma^{\text{pred}}_{mn}} \right) \tag{141}$$

$$\frac{\partial A_{ij}}{\partial \Sigma^{\text{pred}}_{mn}} = \gamma_{ijop} \left(\frac{\partial \bar{a}_{op}}{\partial \Sigma^{\text{pred}}_{mn}} + \frac{\partial A_{op}}{\partial H_{\beta}} \frac{\partial H_{\beta}}{\partial \Sigma^{\text{pred}}_{mn}} \right) \tag{142}$$

The $c_{\alpha\beta}$ and γ_{ijkl} can be found in Appendix I.